Electronic Supplementary Information

Carbon nanodots as a fluorescence probe for rapid, sensitive, and label-free detection of Hg^{2+} and biothiols in complex matrices

Experimental Section

Materials and measurements:

EDTA-2Na·2H2O was purchased from Alfa Aesar and used without further purification. Standard stock solutions of Hg^{2+} ion were prepared with $HgCl_2$ in double-distilled water with the same concentration HCl. Different concentrations of Hg^{2+} ion were obtained by diluting standard stock solutions. All other reagents were of analytical reagent grade and used as received. The UV-Vis absorption spectra and the fluorescence spectra were recorded using a JASCO V-550 UV/Visible and a JASCO FP6500 spectrophotometer (JASCO International Co.,LTD., Tokyo, Japan). The ζ-potential the C-Dots was measured in a Zetasizer 3000HS analyzer. TEM images were recorded using a FEI TECNAI G2 20 high-resolution transmission electron microscope operating at 200 kV. Nanopure water (18.2 MΩ; Millpore Co., USA) was used in all experiments.

Preparation of fluorescent carbon dots (C-Dots):

In a typical procedure, a quartz boat filled with EDTA-2Na·2H2O (AR, 0.5 g) was thrust into a quartz tube and calcined at 400 °C for 2 h in flowing N2. The resulting blank powders were dissolved in acetone (20 mL) and then centrifuged at a high

speed (13000 rpm) for fifteen minutes. Pure luminescent C-Dots powder was obtained by evaporating the upper yellow solution. Then the obtained C-Dots were redissolved in 8 mL double-distilled water as stock solution （66 μg/mL）.

Assay procedure:

4 μL of C-Dots stock solution （66 μg/mL） was mixed with 400 μL of 10 mM Tris-HCl buffer. 5 μL of different concentration of Hg(II) was added, and equilibrated for 5 min at room temperature before the spectral measurements. The fluorescence spectra were recorded under excitation at 360 nm.

For the Cys detection, 4 μL of different concentration of Cys were added to the above mixture solution. After 1 min, the fluorescence spectra were recorded.

FIGURE

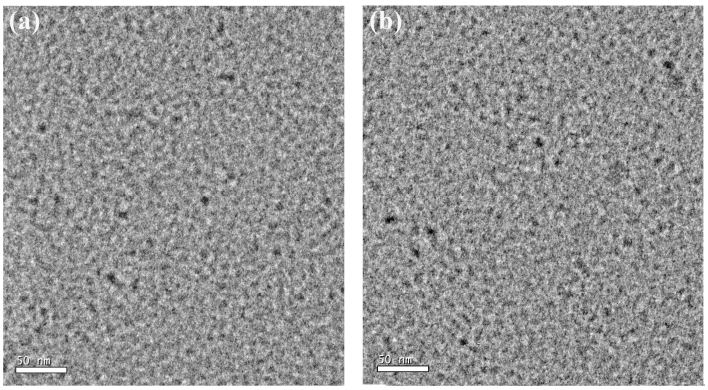

Fig. S1 Transmission electron microscopy (TEM) images of C-Dots in the absence (a) and presence of 5 μM Hg^{2+} (b).

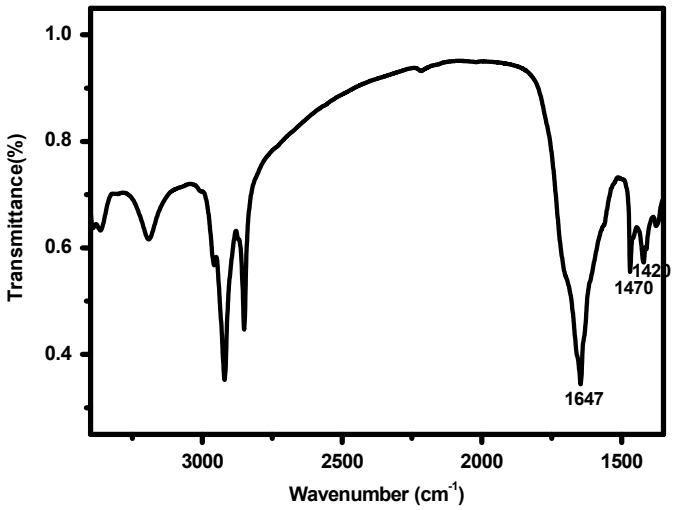

Fig. S2 Fourier transform infrared (FTIR) spectrum of the C-Dots.

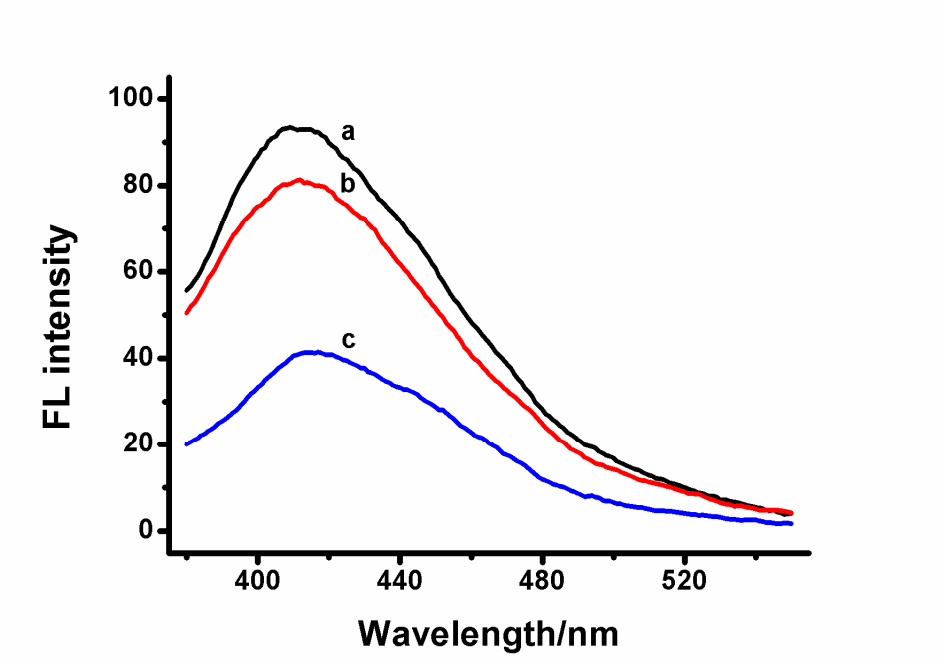

Fig. S3 FL emission spectra of C-Dots in the absence of Hg^{2+} (a) and the presence of Hg^{2+} (40 μM) (b) and FL restoration of the C-Dots/Hg^{2+} system in the presence of Cys (40 μM) (c) in the 10 mM Tris-HCl buffer at pH 8.5.

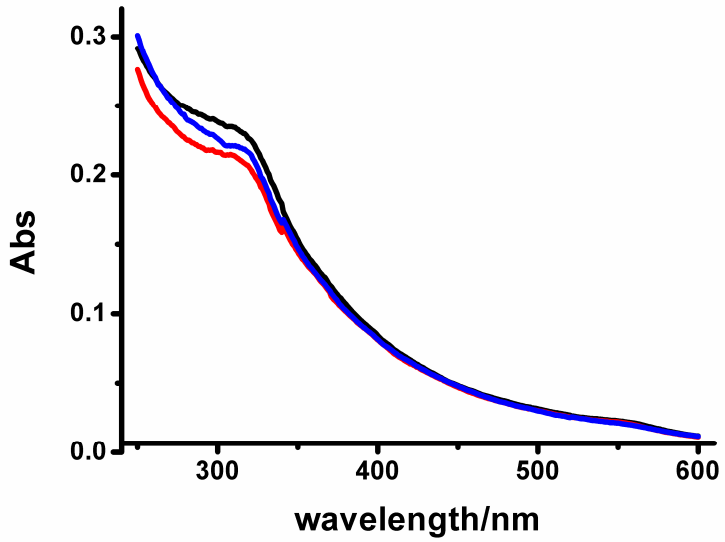

Fig. S4 UV-Vis spectra of C-Dots in the absence of Hg^{2+} (blank lines) and the presence of 40 μM Hg^{2+} (red lines) and UV-Vis restoration of the C-Dots/Hg^{2+} system in the presence of 40 μM Cys (blue lines) in the 10 mM Tris-HCl buffer at pH 8.5.

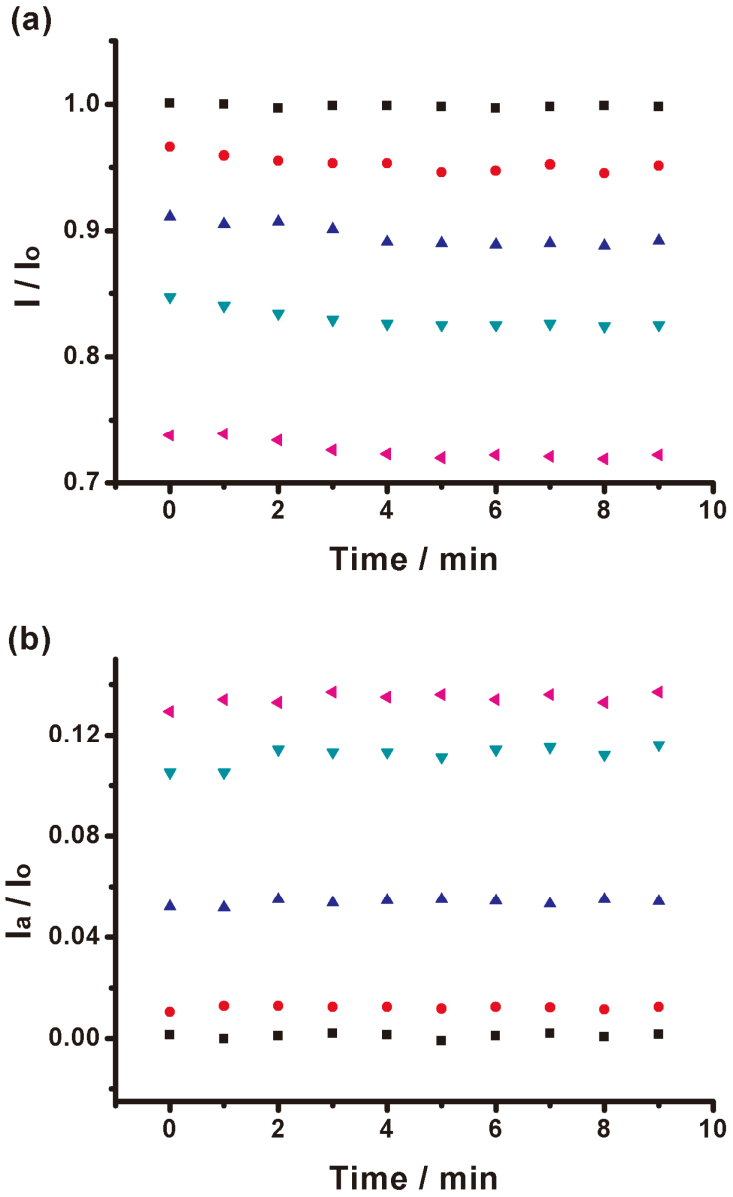

Figure S5 The response time of C-Dots to different concentrations of Hg^{2+} (0 nM, 400 nM, 1 μM, 2 μM) (a) and Cys(0 nM, 100 nM, 400 nM, 1 μM, 2 μM) (b). (I_0, I and Ia were the FL signals of the C-Dots solution without Hg^{2+}, C-Dots solution with Hg^{2+}, C-Dots solution with Hg^{2+} and Cys, respectively)

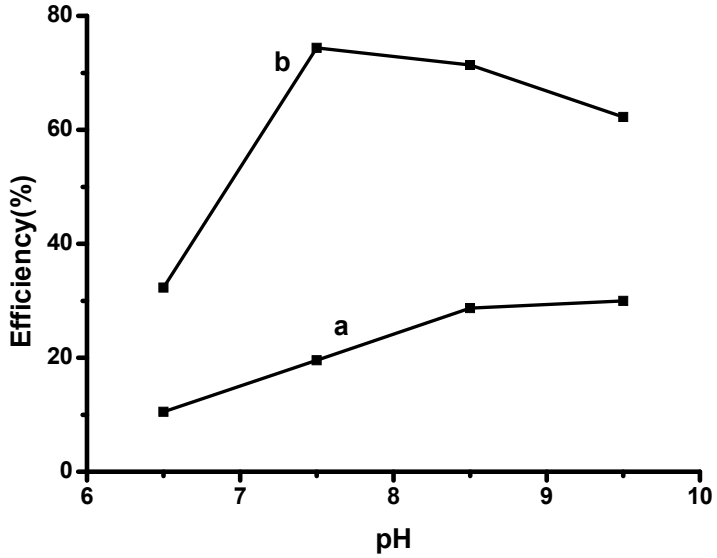

Fig. S6 Plots of the C-Dots FL-quenched efficiency $(I_0- I)/I_0$ by 5.0 μM Hg^{2+} (a) and FL-recovered efficiency $(Ia- I)/(I_0-I)$ at 410nm by 1 μM Cys versus different pH (b).

Table S1 Comparison of different nanoparticle-based methods for Hg^{2+} detection.

Method	**Linear range**	**Detect limit**	**reference**
Fluorescent gold nanoparticle	0.01-10 μM	5 nM	s1
DNA-functionalized gold nanoparticles	0.05-2.5 μM	25 nM	s2
Mononucleotides-stabilized gold nanoparticles	0.02 -6.0 μM	50 nM	s3
Surface-modified CdTe quantum dots	0.012-1.5 mM	4 nM	s4
Au@Ag core-shell Nanoparticles	0.01-0.45 μM	9 nM	s5
Cysteine functionalized Ag nanoparticles	0-55 μM	65 nM	s7
Carbon nanodots	0-3 μM	4.2 nM	Our method

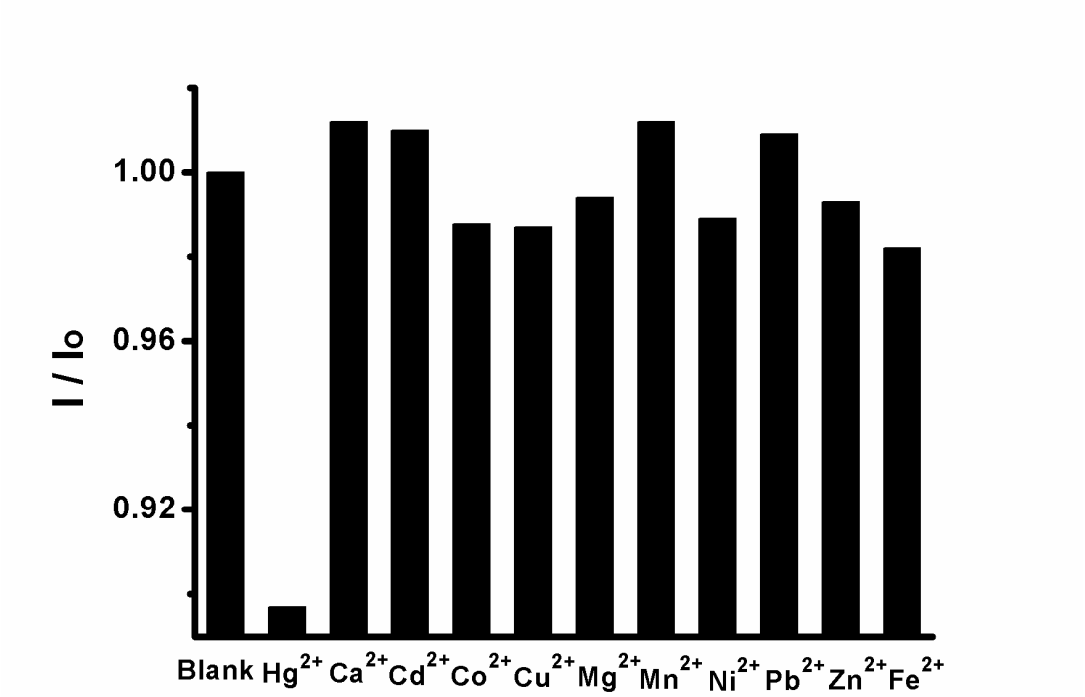

Fig. S7 Selectivity of the Hg^{2+} sensor. All competing ion solutions were 1 μM.

Table S2 Determination of Hg^{2+} in natural water samples.

Samples	**Added Hg(II)(nM)**	**Measured(nM)**	**Recovery(%)**	**RSD(n=3%)**
Lake water	30	30.14	101	1.7
	200	210	105	2.6
Fountain water	30	28.1	94	2.0
	200	194.7	97	2.3
Tap water	30	30.23	101	1.3
	200	213.6	107	1.0

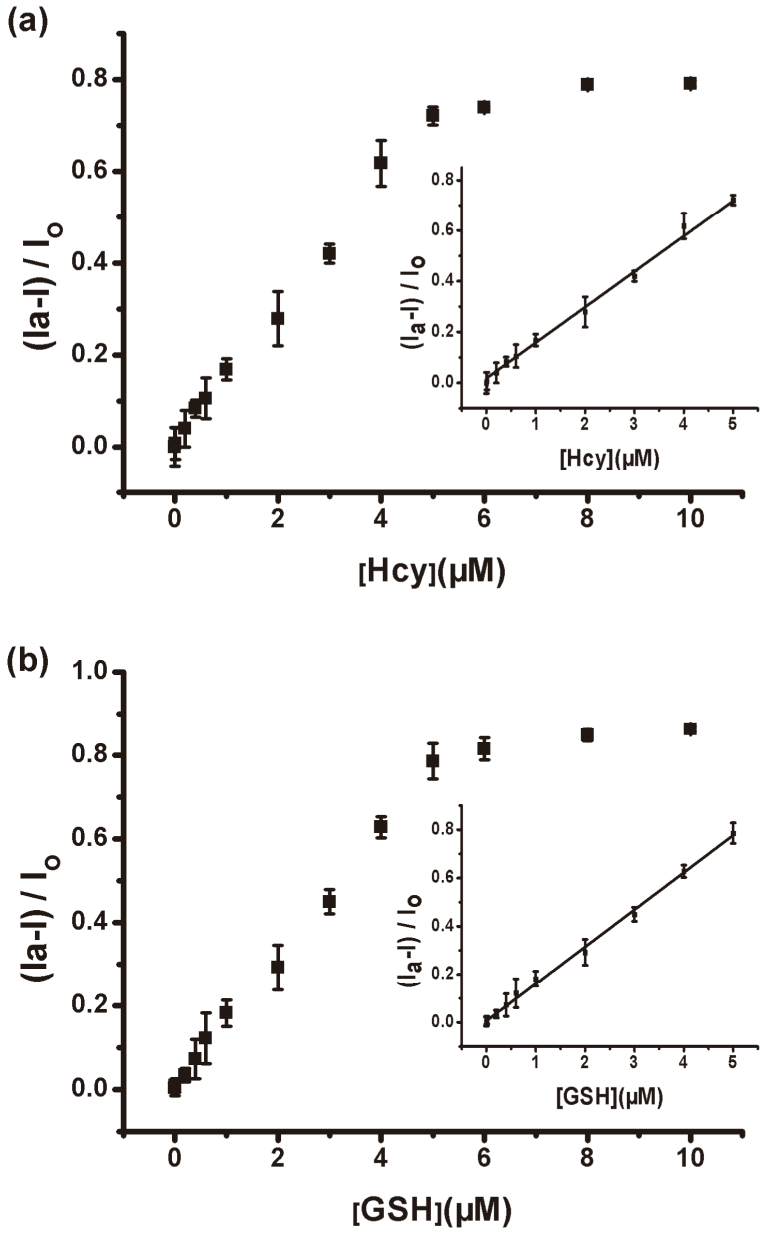

Fig. S8 The relationship between (Ia-I)/I_0 and (a) Hcy (b) GSH from 0.01 to 10 μM, The error bars represent the standard deviation of three measurements. Inset is a linear region. Ia is the recovered FL intensity of C-Dots in the presence of HCy/GSH, I is the FL intensity of C-Dots in the presence of Hg^{2+} (5 μM), and I_0 is the FL intensity of C-Dots at 410 nm, respectively.

Table S3 Comparison of different methods for biothiols detection.

Method	Cys		Hcy		GSH		reference
	linear range	detect limit	linear range	detect limit	linear range	detect limit	
Gold nanoparticle-based near-infrared fluorescent	4.0-250 μM	10 nM	Not given		Not given		s8
CdTe quantum dots-Hg(II) system	2.0-20 μM	0.6 μM	Not given		0.6-20 μM	0.1 μM	s9
CdTe/CdSe quantum dots	0.2-200 μM	131 nM	Not given	26 nM	Not given	26 nM	s10
A fluorescent probe based on fluorescein	Not given	50 nM	Not given	100 nM	0-350 nM	53 nM	s11
Poly(methacrylic acid) templated Ag clusters	6.0-250 μM	20 nM	Not given		Not given		s12
Oligonucleotide-stabilized Ag nanoclusters	8.0-100 nM	4.0 nM	0.6-2 μM	0.2 μM	8.0-100 nM	4.0 nM	s13
DNA/Ligand/Ion-Based	2.5-110 nM	5.1 nM	Not given		Not given		s14
Carbon nanodots/Hg^{2+}	0.01-5 μM	4.9 nM	0.01-5 μM	6.1 nM	0.01-5 μM	8.5 nM	Our method

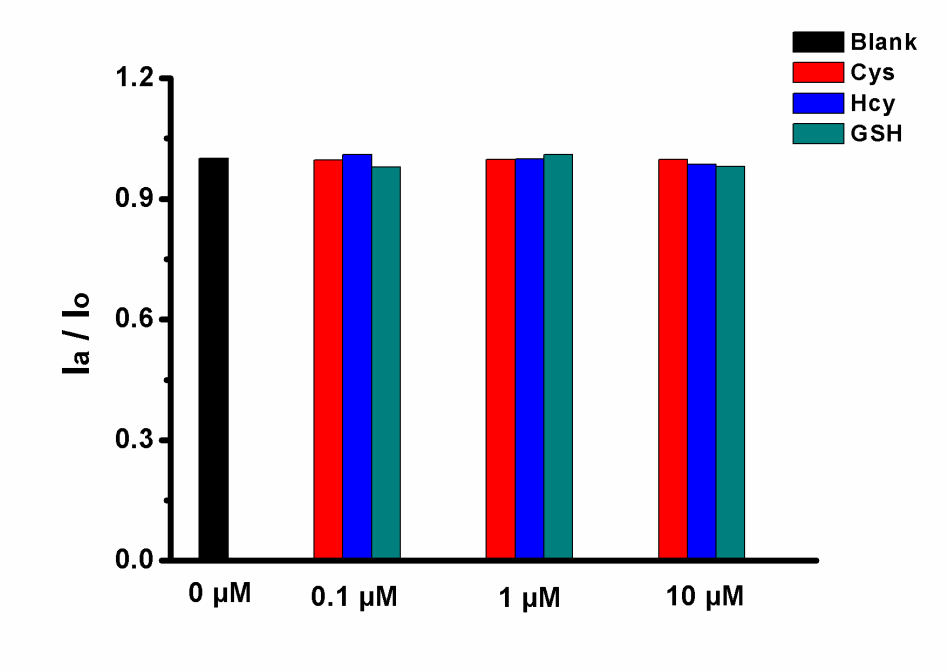

Fig. S9 FL response of C-Dots solution in the presence of different concentrations of biothiols.

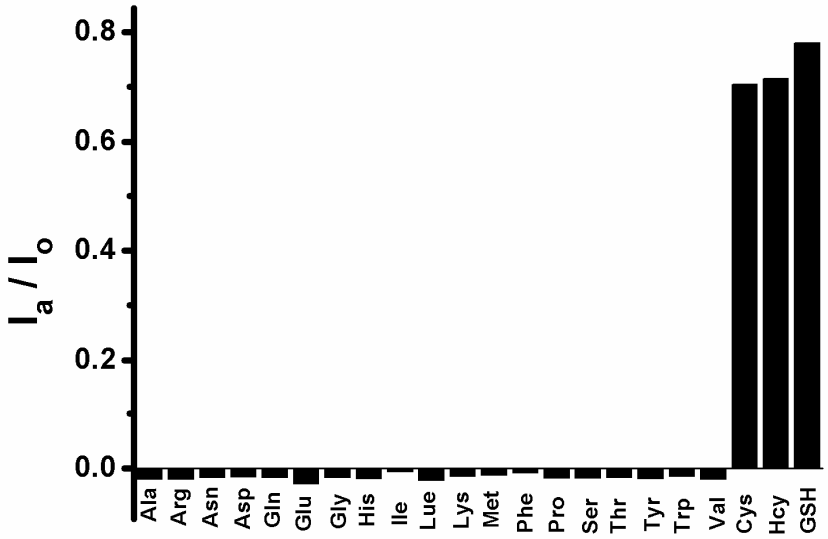

Fig. S10 FL response of C-Dots/Hg^{2+} solution towards 19 essential amino acids at a concentration of 5 μM.

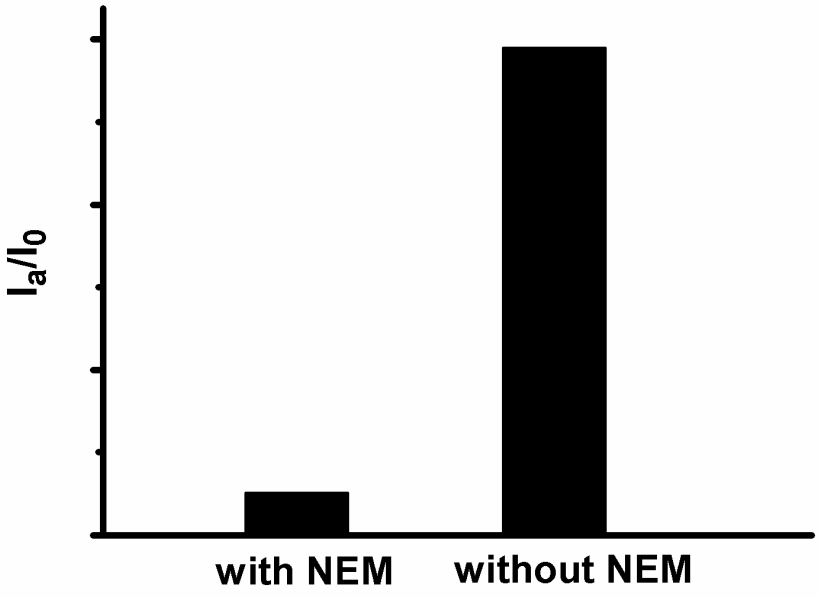

Fig. S11 FL response of C-Dots/Hg^{2+} to serum with or without pretreatment by thiol blocking agent, NEM.

Table S4 Determination of biothiols in fetal bovine serum （fetal bovine serum was diluted with buffer before detection）.

Determined biothiol (μ M)	Added Cys (μ M)	Measured (μ M)	Recovery (%)	RSD (n=3, %)
168.6	50	229.6	104.9	2.38
168.6	100	279	96.1	3.1

Supporting References

(s1) C. C. Huang, Z. Yang, K. H. Lee and H. T. Chang, *Angew. Chem. Int. Ed.,* 2007, **46**, 6824–6828.

(s2) C. W. Liu, C. C. Huang and H. T. Chang, *Langmuir*, 2008, **24**, 8346–8350.

(s3) Y. Xu, L. Deng, H. Wang, X. Ouyang, J. Zheng, J. Li and R. Yang, *Chem. Commun.*, 2011, **47**, 6039–6041.

(s4) Y. Xia, C. Zhu, *Talanta*, 2008, **75**, 215–221.

(s5) S. Guha, S. Roy and A. Banerjee, *Langmuir*, 2011, **27**, 13198–13205.

(s6) C. Jiang, Z. Guan, S. Y. R. Lim, L. Polavarapu and Q. Xu, *Nanoscale*, 2011, **3**, 3316–3320.

(s7) L. Shang, J. Yin, J. Li, L. Jin and S. Dong, *Biosens. Bioelectron*., 2009, **25**, 269–274.

(s8) B. Han, J. Yuan and E. Wang, *Anal. Chem*., 2009, **81**, 5569–5573.

(s9) Y. Zhang, Y. Li and X. Yan, *Anal. Chem*., 2009, **81,** 5001–5007.

(s10) X. Chen, S. K. Ko, M. J. Kim, I. Shin and J. Yoon, *Chem. Commun.*, 2010, **46**, 2751–2753.

(s11) L. Shang, S. Dong, *Biosens. Bioelectron*., 2009, **24**, 1569–1573.

(s12) B. Han and E. Wang, *Biosens. Bioelectron*., 2011, **26**, 2585–2589.

(s13) F. Pu, Z. Huang, J. Ren and X. Qu, *Anal. Chem*., 2010, **82**, 8211–8216.